Hindawi
Journal of Nanomaterials
Volume 2020, Article ID 4147357, 11 pages
https://doi.org/10.1155/2020/4147357

Research Article

Green Synthesis of ZnO-GO Composites for the Photocatalytic Degradation of Methylene Blue

Yi Lin,[1] Ruoyu Hong,[1] Huaiyin Chen,[1] Di Zhang,[1] and Jinjia Xu[2]

[1]*College of Chemical Engineering, Fuzhou University, Fuzhou 350002, China*
[2]*Weldon School of Biomedical Engineering, Birck Nanotechnology Center, Center for Implantable Devices, Purdue University, West Lafayette, IN 47906, USA*

Correspondence should be addressed to Ruoyu Hong; rhong@fzu.edu.cn

Received 18 February 2020; Revised 5 April 2020; Accepted 20 April 2020; Published 18 August 2020

Guest Editor: Hai Nguyen Tran

Beneficial from the excellent optical performance of zinc oxide (ZnO) nanocrystals and the absorption properties of graphene oxide (GO), the nanocomposites of ZnO and GO with synergistic photocatalytic effects were prepared by a precipitation method, in which GO is utilized as the catalyst carrier. The prepared composites were characterized by X-ray diffraction, X-ray photoelectron spectroscopy, UV-vis spectroscopy, field emission scanning electron microscopy, and transmission electron microscopy and also performed photocatalytic activity for the nanocomposites. The results show that ZnO is uniformly loaded on the surface of GO assisted by an effective interface coupling. Due to interface coupling between ZnO and GO, electrons can be directly transferred from the valence band of ZnO to GO. The photodegradation efficiency of the composites reaches to 97.6%, and the first-order reaction rate constant of photodegradation is calculated to be 0.04401 min^{-1}. The novel ZnO-GO composites with excellent photocatalytic performance display promising potential applications in the field of photocatalysis and will provide a new platform for building next-generation graphene-based semiconductor composites.

1. Introduction

Along with the rapid development of the industrialization, the issue of water pollution becomes serious and causes detrimental effects to environment. According to recent reports, many industries discharge about 70% of their waste products into water directly without any refinements [1]. How to deal with water pollution by high-efficiency, energy-saving, and low-cost approaches needs to be solved urgently. Removal of organic pollutants is of great significance for water conservation. As an inexhaustible, safe, reliable energy source, solar energy is considered as the most ideal green and clean energy for human beings [2]. The development of catalysts for effective photocatalytic degradation of organic dyes in waste water is one of the promising means of water purification and gradually becomes a hot research topic in the field of environmental protection.

Since the first demonstrated single crystal TiO_2 for water splitting to H_2 published in 1972 by Fujishima and Honda [3], photocatalysis has attracted enormous attention of many researchers in various fields including chemistry, physics, materials, and environmental protection. In the past few decades, scientists have made considerable efforts to develop new semiconductor photocatalysts [4, 5]; many inexpensive, efficient, and stable photocatalysts have been prepared and used in photochemical sewerage treatments, such as metal oxides (TiO_2 [6], ZnO [7, 8]), sulfides [9], and oxynitrides [10]. ZnO is a kind of *n*-type semiconductor photocatalyst with a wide band gap, high electron excitation binding energy (about 60 meV at room temperature), favorable electric and photonic properties, and oxidation resistance. ZnO has been considered as a substitute for TiO_2 for the high catalytic activity, simple preparation process, relatively low cost, and avirulence [11]. In particular, ZnO can be used to resist bacteria and shield ultraviolet radiation, as reported by our previous study work [12–14].

ZnO has low cost and it can be applicable in wide temperature range, so it has been extensively used in environmental treatment [15]. However, ZnO nanoparticles have some drawbacks, such as ununiformed dispersion, high resistivity,

difficulty in fixing, and the facile combination of photogenerated electron-hole pairs [16]. As a result, ZnO can only be activated by UV irradiation and the light quantum efficiency is low. In order to prevent the recombination of electron and hole pairs and enhance the photocatalytic performance in the UV region by narrowing the band gap of ZnO semiconductors, much research has been done on functionalizing synthesized ZnO with other materials [17], such as making the nanocomposites with graphene oxide (GO) and reduced graphene oxide (rGO) [18–20].

GO is one of the two-dimensional (2D) materials with high specific surface area, excellent adsorption effect, and good catalytic effect and thermodynamic properties [21], which can improve the catalytic effect of photocatalysts. For the ZnO-GO composite photocatalyst, ZnO and GO act as the photocatalyst and the material for electron-acceptor/-transport, respectively, which promote the migration of photogenerated electrons and hinder the electron-hole recombination in a large extent [22]. The fact of improvement in photocatalytic efficiency is that the photogenerated electrons migrating to the surface can react with the hybrid GO layer, which suppresses the recombination of photogenerated electrons and holes to promote the effective separation of photogenerated electrons and holes [23]. Particularly, for the photodegradation of organic dyes, GO plays a significant role in enhancing the photodegradation efficiency of photocatalysts, due to the strong adsorption effect between GO and various organic dyes [24].

In this study, the ZnO-GO nanocomposites were successfully synthesized by a facile precipitation method and further used as the photocatalyst for the degradation of methylene blue (MB) dye. The functional groups and hydroxyl, carboxyl, and epoxy groups of GO provided anchor sites for the growth of ZnO nanocrystals to form the flake-like nanocomposites. With the help of comprehensive characterization methods including XRD, XPS, and SEM, it can conclude that the ZnO has been successfully decorated on the surface of GO. The as-prepared ZnO-GO composites exhibit more excellent and stable photocatalytic performance than pure ZnO, ascribed to the fact that GO sheets collected and transmitted the electrons, thereby inhibiting the recombination of electron-hole pairs. Compared with other previous reports on ZnO-GO composites catalysts, most of which use light sources with hundreds of W or higher power to excite the catalysts for photocatalytic reactions [25]; the as-prepared ZnO-GO catalysts in this study showed higher catalytic activity under the light source of 50 W mercury lamps. This effective photocatalyst is an outstanding candidate for catalysts in photocatalytic degradation of organic dyes.

2. Experimental

2.1. Materials. Ethanol (99.9%), zinc sulfate heptahydrate ($ZnSO_4{\cdot}7H_2O$), sodium hydroxide (NaOH), and methylene blue (MB) were purchased from Sinopharm Chemical Reagent Co., Ltd. Graphene oxide (GO) was prepared via the modified Hummer method and spray drying to obtain a brown powder. Deionized water was used throughout the experiments.

2.2. Synthesis. All the chemicals were analytic grade reagents without further purification. The solvent medium used for the reaction system was deionized water. The preparation procedure of ZnO and ZnO-GO nanostructures consists of two steps: (1) synthesis of precursor, $Zn(OH)_2$, for the growth of ZnO nanostructures and (2) hydrothermal growth of ZnO and ZnO-GO structures in aqueous medium.

2.2.1. Synthesis of Precursor. The precipitation method was applied for the preparation of nano-ZnO powders. 28.76 g of $ZnSO_4{\cdot}7H_2O$ and 8.00 g of NaOH were, respectively, dissolved in 50 mL deionized water to give 2 M $ZnSO_4$ and 4 M NaOH solutions, respectively. The $ZnSO_4$ solution was poured into a 250 mL three-necked flask, and then the NaOH solution was added dropwise with the rate of 2 mL/min under vigorously stirring (250 rpm) at 25°C. After that, the reaction was continued for another 30 min, and then the precipitate was filtered, washed for several times with deionized water, and then placed in a Buchner funnel and sealed and placed overnight at room temperature to obtain the precipitated precursor.

2.2.2. Growth of ZnO Nanostructure and ZnO-GO Nanocomposite. Firstly, 2.00 g of precursors and different amounts of GO (50 mg, 100 mg, 150 mg) powders were put into a conical flask. Then, 1 M NaOH aqueous solution (70 mL, 80 mL, 90 mL, 100 mL) was added into the flask and syringed into the flask with vigorous stirring for 1 h. The suspension was ultrasonically treated in an ultrasonic bath for 1 h at room temperature, before it was transferred to a 250 mL three-necked flask. The reaction was proceeded with vigorous stirring (250 rpm) for 2 h at 60°C and kept for another 6 h at 80°C. The precipitations were collected, then washed several times with deionized water and anhydrous ethanol after prior to cooling down to room temperature, and then dried at 60°C under vacuum for 12 h. Finally, the precipitations were calcined in an oven at different temperatures (300°C, 350°C, 400°C, 450°C, 500°C) for 3 h in N_2 atmosphere and milled to obtain ZnO nanoparticles; the heating rate is 5°C/min.

2.3. Photocatalytic Activity Tests. The photocatalytic performance of the prepared photocatalysts, ZnO nanoparticles, and ZnO-GO composites was evaluated by photodegradation of methylene blue (MB) under simulated ultraviolet light supplied by 50 W high-pressure mercury lamp at room temperature. In a typical reaction, 20 mg of the photocatalyst was dispersed in 100 mL of MB aqueous solution (0.015 g/L, i.e., 4.01×10^{-5} M) under magnetic stirring. The distance between the experimental setup and the light source was set as 7 cm for all the photodegradation experiments. Before photodegradation experiments, the mixture of catalyst and dye was stirred in the absence of light for 1 h until reaching adsorption-desorption equilibrium. The mixture was exposed to the light derived from high-pressure mercury lamp under continuous magnetic stirring. 3 mL of the mixture was taken out every 10 min and centrifuged to remove the catalysts for the absorbance change measurements by using UV-vis spectrophotometer. The reusability

and photostability of ZnO-GO nanocomposites were investigated for MB degradation for five cycles. The ZnO-GO catalysts were collected and washed for the next cycle degradation. The obtained powder was dried at 60°C for 12 h. The concentration changes of MB dye in solution were determined by the characteristic absorption of MB at the wavelength of 665 nm.

2.4. Characterization. The crystal structure of samples was characterized by the mean of X-ray diffraction (XRD) using a PANalytical X'Pert PRO X-ray diffractometer with Cu Kα irradiation source ($\lambda = 1.5406$ Å) from 5° to 80° at a rate of 0.02°/s. The morphologies of the resultant products were measured with a FEI Tecnai G2 F20 transmission electron microscope (TEM) with an acceleration voltage of 200 kV and Hitachi S-4800 field emission scanning electron microscopy (FE-SEM). The surface properties of the powders were characterized by a VG ESCALAB 250 X-ray photoelectron spectrometer (XPS), with a monochromatic Al Kα X-ray source ($h\nu = 1486.6$ eV). The UV-vis spectra were measured using a Persee TU-1900 UV-vis spectrophotometer, in the wavelength range of 200-800 nm.

3. Results and Discussion

3.1. Structural Analysis. In order to gain the crystal structure information of ZnO and ZnO-GO as well as the influences from different preparation conditions, the XRD measurements of the photocatalysts were conducted, as shown in Figure 1. The characteristic peaks at $2\theta = 31.7°$, 34.4°, 36.2°, 47.5°, 56.7°, 63.0°, 66.4°, 68.1°, and 69.3° were observed from the XRD patterns of ZnO and ZnO-GO nanocomposites annealed at 450°C, corresponding to the planes (100), (002), (101), (102), (110), (103), (200), (112), and (201), respectively (Figure 1(a)), indicating the existence of ZnO with hexagonal wurtzite phase (JCPDS No. 361451). No existence of other phases or impurity was found, indicating the high purity of catalysts [26–28]. It is notable that the characteristic diffraction peak of GO at $2\theta = 12.6°$ was not found in the XRD pattern of ZnO-GO, which was probably because ZnO crystals were covered by limited amounts of GO that changed its structure [29]. According to related literatures [30], the presence of grain boundaries in ZnO and ZnO-GO nanocomposition can be proved owing to the existence of amorphous superficial and intergranular layers between ZnO and ZnO-GO photocatalysts (unobservable in XRD patterns).

In addition, the influence of adding amounts of NaOH on the ZnO structure was been studied. It is clearly observed from Figure 1(b) that the diffraction peak intensity of the ZnO increases first and then decreases upon increasing the amounts of NaOH; moreover, the diffraction peaks become the sharpest when the adding amount of NaOH is 80 mL. Figure 1(c) shows the effect of adding amounts of GO on the ZnO-GO nanocomposite structure. We found that the diffraction peak intensity decreases with the increase adding amounts of GO.

3.2. Component Analysis. The chemical state of element component for ZnO-GO nanocomposites annealed at 450°C was explored by X-ray photoelectron spectroscopy (XPS), and the

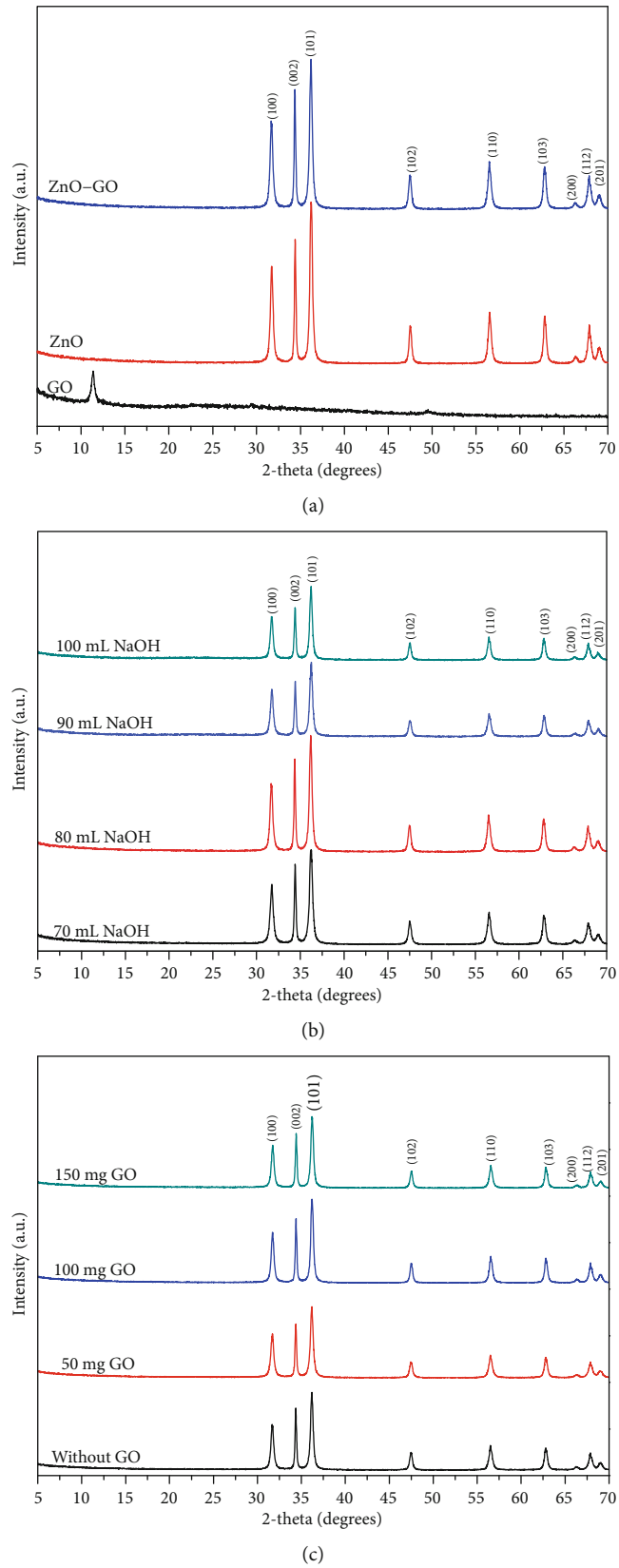

Figure 1: XRD patterns of (a) GO, ZnO, and ZnO-GO, (b) bare ZnO prepared under varying NaOH additions, and (c) ZnO-GO nanocomposite prepared under varying GO additions.

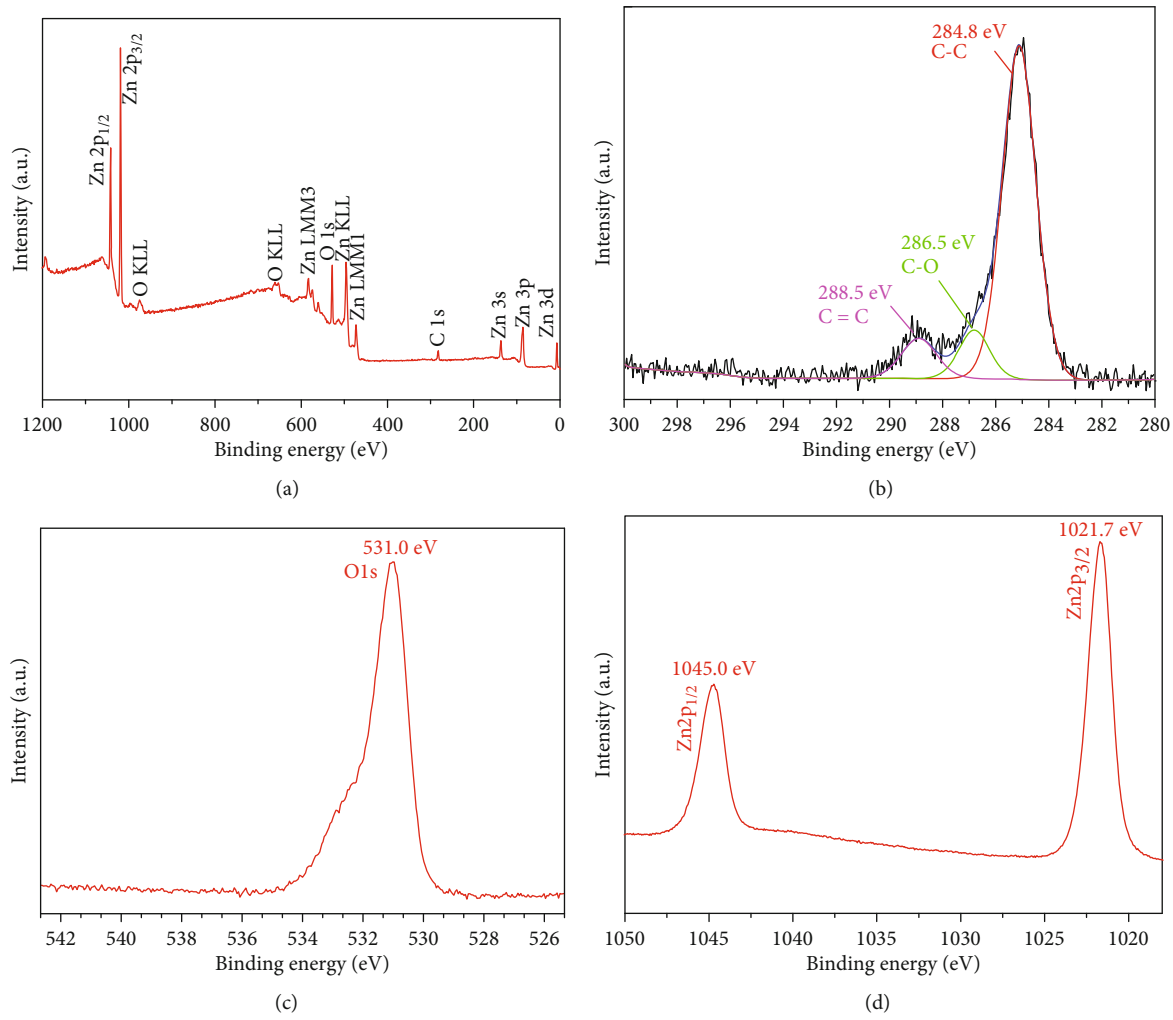

Figure 2: (a) XPS spectra, (b) C1s region for GO-ZnO nanocomposite, (c) O1s region, and (d) high-resolution spectra of Zn2p region.

interfacial interaction information among compositions are shown in Figure 2. The wide range analysis pattern of ZnO-GO nanocomposites is comprised of C1s (284.8 eV), O1s (531.0 eV), and Zn2p (1021.7 eV), without other elemental peaks. Figure 2(b). shows deconvoluted C1s XPS spectrum in three distinct peaks at 284.8 eV, 286.5 eV, and 288.5 eV, respectively, which all contributed from graphene oxide [31]. The 284.8 eV peak is ascribed to the sp2 carbon atom of C-C bond, and the 286.5 eV peak is represented by C-O bond contributed by the epoxy and hydroxyl groups. The carboxylate C=C covalent bond is assigned at the peak around 288.5 eV [32, 33]. Figure 2(c) depicts the O1s exact curve which can be fitted to the peak appeared at around 531.0 eV. It is facilitated by the chemisorbed oxygen atom and lattice oxygen in nanocomposites [34]. As shown in Figure 2(d), the bounding energy locations of 1045.5 eV and 1021.7 eV conform to the present of two atomic states, $Zn2p_{1/2}$ and $Zn2p_{3/2}$ corresponding to the electronic configuration of Zn^{2+} [35].

3.3. Morphological Analysis. The FE-SEM was used to study the morphologies of the as-prepared GO, ZnO, and ZnO-GO nanomaterials, as shown in Figure 3. Figure 3(a) displays GO which has a carpet-like pattern, probably because of residual bound moisture and the hydroxyl, epoxy, and carboxyl functional groups adhered to the surface of GO [36]. The graphene sheets are not perfectly flat but intrinsically microscopic roughening and out-of-plane deformations (wrinkles). Besides, some dispersed GO sheets could connect randomly to each other that brought about a porous structure with numerous cavities or holes, which provides additional possibilities to form ZnO-GO nanohybrid between precursor and GO. Figure 3(b) clearly shows that ZnO nanoparticles appear as granule-like nanostructures and the powder aggregation at different levels. It can be seen from Figure 3(c) that the surface of GO is covered rigorously by ZnO crystals, demonstrating a good combination between GO sheet and ZnO nanoparticles. The ZnO-GO catalyst shows a cross-linked flaky structure and excellent dispersibility without agglomeration, and the structure presents an average thickness of about 20 nm. The SEM images of the ZnO-GO nanocomposites after annealing treatment at 450°C are shown in Figure 3(d). It can be observed obviously that the ZnO-GO nanocomposites collapsed into a smaller average sizes. It can be seen that the calcined samples have

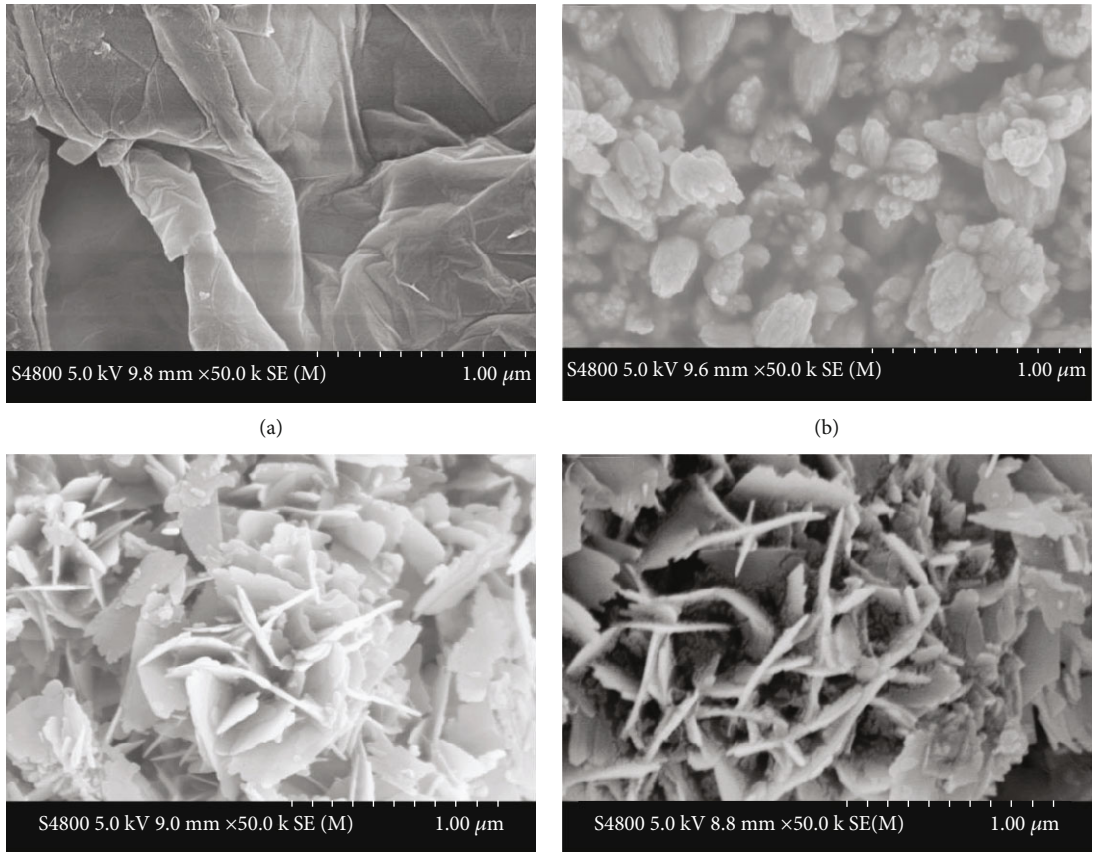

Figure 3: SEM images of (a) GO, (b) ZnO, (c) ZnO-GO nanocomposite, and (d) ZnO-GO nanocomposite annealed at 450°C.

better dispersion. To a certain extent, such samples have a larger specific surface area, which is conducive to the improvement of photocatalytic activity. As reported, the large specific surface area can further improve the catalytic activity for photodegradation [37]. Hence, it is reasonable to form the ZnO-GO catalyst with tunable sizes and specific surface areas.

The transmission electron micrograph (TEM) images of the GO, ZnO, and ZnO-GO nanocomposites annealed at 450°C are shown in Figure 4. Figure 4(a) shows high-magnified image of pure GO having wrinkled-like structures, which provides a chemical reaction condition for ZnO crystal deposition. The wide carrier GO could decrease the agglomeration formation rate of ZnO and further improve the charge separation and photodegradation activity [38]. Figure 4(b) illustrates the ZnO nanoparticles with a lattice space of 2.60 Å corresponding to (101) diffraction, which is consistent with XRD results. The images shown in Figure 4(c) demonstrate the lattice plane in (101) directions of wurtzite structure from one particle of ZnO-GO nanocomposite, implying that ZnO crystal deposited on GO sheet firmly. The conclusions obtained above are in good accordance with the results calculated from XRD analysis. The interaction between ZnO and GO sheets may be ascribed to the existence of epoxide accompanied by the hydroxide groups on GO surface that gives activated reaction sites of immobilization for ZnO crystals [39]. The above description shows only lattice space or direction, while the specific area axis of the hybridization structure described above cannot be defined. Under the present investigation, we can infer that the substance detected by TEM belongs to ZnO wurtzite structure from the identified lattice space or direction. The base GO does not affect the crystalline structure of ZnO, due to that the crystalline of ZnO deposited on GO is consistent with ZnO.

3.4. Optical Properties. As a comparison, the optical properties of GO, ZnO, and ZnO-GO nanocomposites annealed at 450°C were detected by UV-vis spectroscopy as expressed in Figure 5. It is clearly observed that an absorption peak centered at 231 nm is assigned to π-$\pi*$ transitions of aromatic C=C bonds in GO. In addition, a shoulder peak near 300 nm reflected to n-$\pi*$ transitions of aromatic C=O bonds [40]. Due to the transition of the electron from the valence band to the conduction band (O_{2p}-Zn_{3d}), the UV-vis absorption of the sample might be demonstrated at around 375 nm, which can be attributed to the intrinsic band gap absorption of ZnO [41, 42]. The UV-vis absorbance of ZnO-GO hybridization is heightened as displayed in the profile. Due to the absorbance of GO, the increase of surface electric charge of the oxides and the compounds forms change of electron-hole pair under UV and visible light [43]. The band gap of semiconductor catalyst can be calculated by the Kubelka-

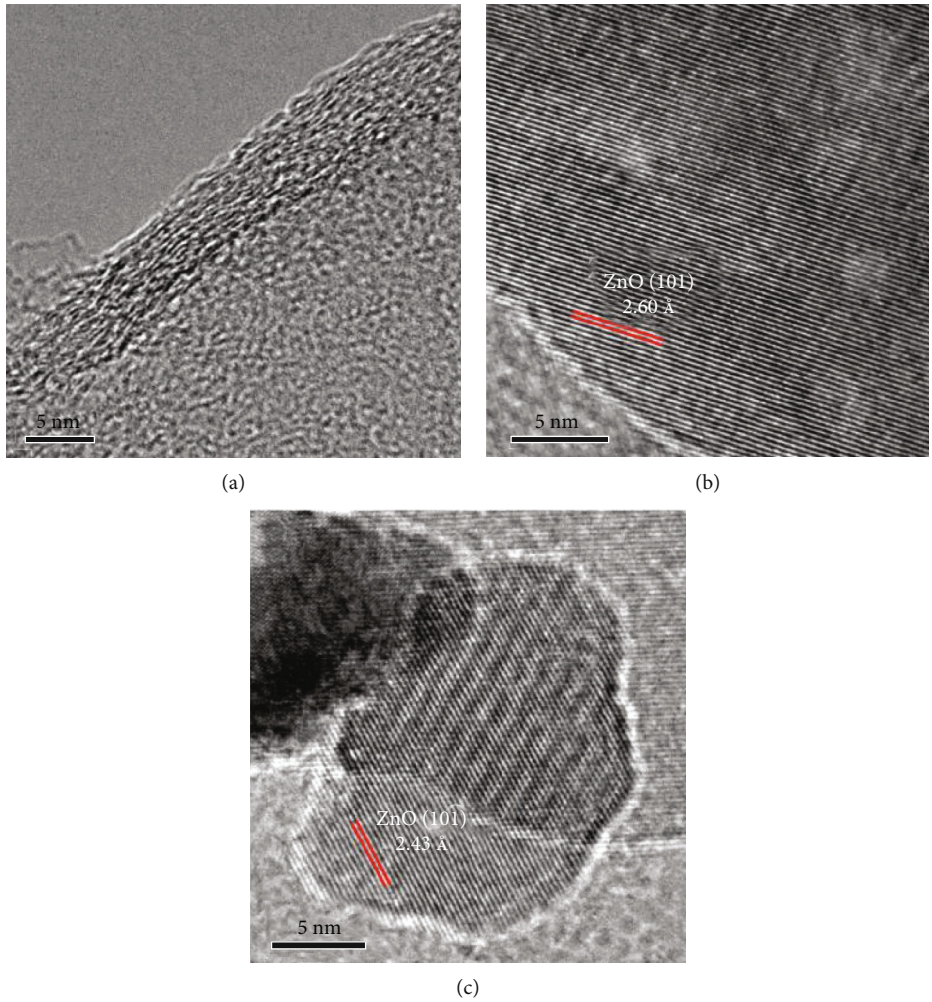

Figure 4: TEM images of (a) GO sheet, (b) ZnO, and (c) ZnO-GO nanocomposite.

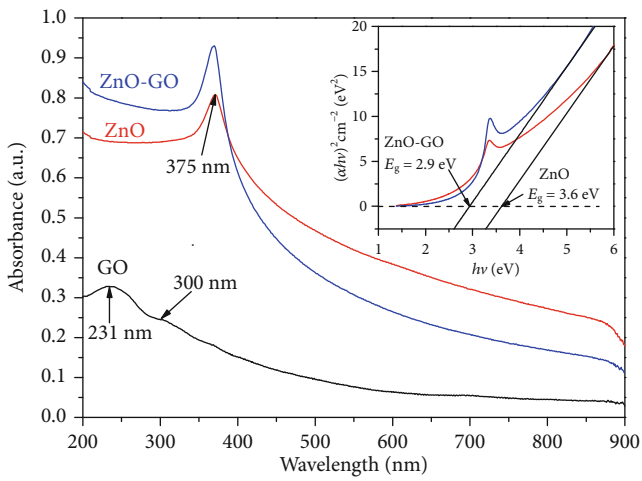

Figure 5: UV-vis absorption spectra of GO, ZnO, and ZnO-GO nanocomposites; the inset figure suggests the corresponding $(\alpha h\nu)^2$ versus the $h\nu$ for ZnO crystal and ZnO-GO nanocomposites.

Munk method [44]. The absorption coefficient (α) versus photon energy ($h\nu$) for the direct band gap semiconductor can be expressed as follows:

$$\alpha h\nu = A\left(h\nu - E_g\right)^{\eta}, \tag{1}$$

where α can be determined according to Kubelka-Munk theory, h is Planck's constant ν is the frequency of light, A is the absorption constant for direct transitions, E_g is the energy band gap value, and η is an index which features the process of optical absorption, and it is equal to 1/2, 2, 3/2, and 3 theoretically for direct allowed, indirect allowed, direct forbidden, and indirect forbidden transitions, respectively. It is well known that ZnO is one of the direct band gap semiconductors. The inset figure in Figure 5 shows the plots of the $(\alpha h\nu)^2$ versus photon energy ($h\nu$). The energy band gap for bare ZnO is calculated to be 3.6 eV, while energy band gap of ZnO-GO nanocomposite drops down to 2.9 eV. Accordingly, the existence of GO carrying ZnO can enhance the light absorption and widen the ultraviolet region range as described in ZnO-GO nanocomposites.

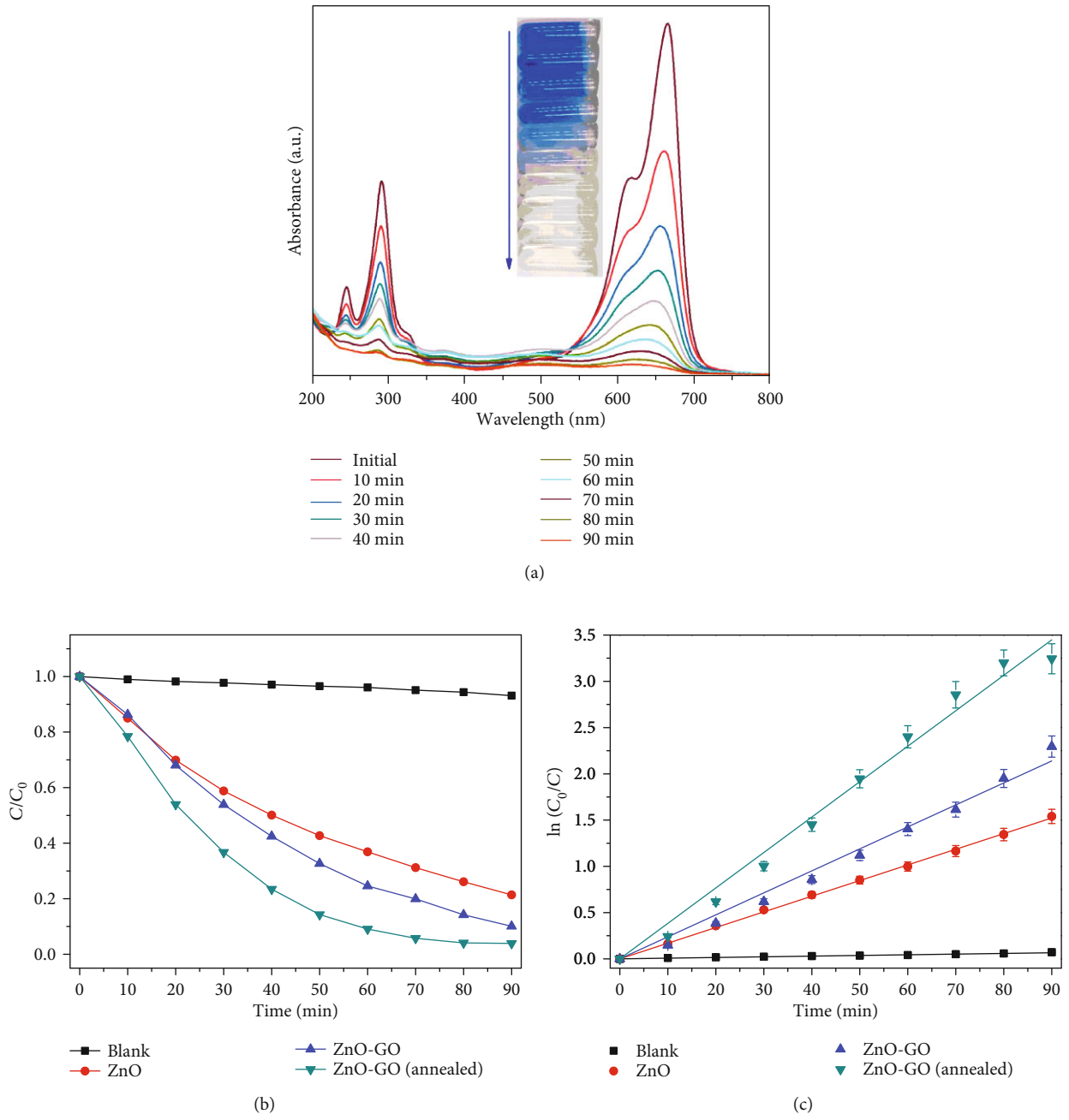

Figure 6: (a) UV-vis spectral changes of MB dye as a series of interval illumination times, (b) photocatalytic degradation of MB by as prepared ZnO-GO nanocomposites, and (c) kinetic curves of various as prepared catalysts.

3.5. Photocatalytic Properties. To evaluate the activities of photocatalyst, pure ZnO semiconductors and ZnO-GO nanocomposites obtained in various preparation processes were used for the degradation of molecular model pollutant and methylene blue (MB). The MB dye and catalyst were mixed by magnetic stirring continuously for 1 h in dark before photodegradation to ensure the system under adsorption-desorption equilibrium. Then, under ultraviolet and visible light emitted by the high-pressure mercury lamp irradiation at different interval times, the absorbance of the solution was measured after centrifugation. As displayed in Figure 6(a), the UV-vis absorbance intensity of MB decreases with the irradiation time increasing, which confirms the MB molecules were degraded effectively by ZnO-GO nanocomposites. Figure 6(b) depicts the real-time changes of MB concentration with the increase of irradiation time for all monitored catalysts under ultraviolet and visible light radiation. In the case of pristine MB (without ZnO or ZnO-GO nanocomposites), there is a slight decrease in absorbance intensity of MB upon the UV-vis light irradiation, which infers that the MB is hardly degraded in the absence of catalyst under UV light. The degradation rate in blank photocatalysis experiment is only 6.8%. It is clear that, for both ZnO and ZnO-GO nanocomposites, MB concentrations

Table 1: The comparison table for photocatalytic MB degradation performance of ZnO/GO composite with other materials reported is as follows.

Catalyst	Light source (W)	Dye concentration/100 mL (mg/L)	Catalyst mass (mg)	Reaction time (min)	Degradation rate (%)	Reference
ZnO/GO	160	20	50	180	93	[25]
ZnO/GO	300	10	50	120	99	[21]
rGO/TiO_2/ZnO	300	0.3	10	120	92	[48]
ZnO/GO	50	20	20	90	97.6	This study

decrease with the increase of irradiation time, indicating all these materials have the photocatalytic activity for degradation of MB. About 93.5% of MB dye was degraded by ZnO-GO nanocomposite within 90 min, and the degradation rate increased to 97.6% after being annealed at 450°C, while only 80.9% of MB dye was degraded by ZnO catalyst. The catalytic activity of ZnO for MB photodegradation is enhanced after loading ZnO on GO sheet surface since the ZnO-GO nanocomposite photocatalysts possess higher catalytic activity. The higher photodegradation efficiency was ascribed to the availability of more active photocatalyst surface for dye absorption, enhanced photoabsorption, and subsequent reactive oxygen species (ROS) generation [45]. This is because the existence of GO hinders the recombination of electron-hole pairs, enhances the absorption of MB, and widens the ultraviolet region range for catalysts [46, 47]. In our study, the impurities on the surface of the catalyst were removed by calcination, and the size of the catalyst was reduced; however, when the temperature was too high, the small-sized catalysts were easy to agglomerate. Combining the influence of various factors, we degraded MB by photocatalyzing the sample after calcination. Upon annealed at 450°C, the ZnO-GO nanocomposites have the highest photocatalytic activity, suggesting that the small-sized crystal nanostructures of ZnO-GO lead to large surface area, so we regard 450°C as the most suitable heat treatment temperature. The excellent adhesion of ZnO onto the surface of GO in the catalyst provides efficient electronic transmission channels since electron-hole pairs are difficult to compound.

In the most previous researches, the experiments of organic dye photodegradation have always been performed in dye aqueous dispersions; the whole system was illuminated by high-power UV-visible light sources for a long time. Table 1 shows the comparison of photocatalytic MB degradation performance of our prepared ZnO/GO composite with other materials reported. Mohamed et al. [25] reported on photocatalysis of ZnO/GO, detecting the MB degradation under visible light illumination using a 160 W Hg lamp; in their study, a solution of 20 mg/L (100 mL) of MB and 50 mg of catalyst were used. Their results show that above 93% MB could be degraded after 180 min by ZnO/GO composite. In addition, considering another investigation by Xue and Zou [21], they carried out the study on ZnO-graphene composite for photocatalytic decolorization of MB; 100 mL of a MB aqueous solution (10 mg/L) and 50 mg of ZnO/graphene were mixed, with irradiation under UV light source emitted by a 300 W xenon lamp; they report 99% of degradation in 120 min for ZnO/rGO; the first-order rate constant is

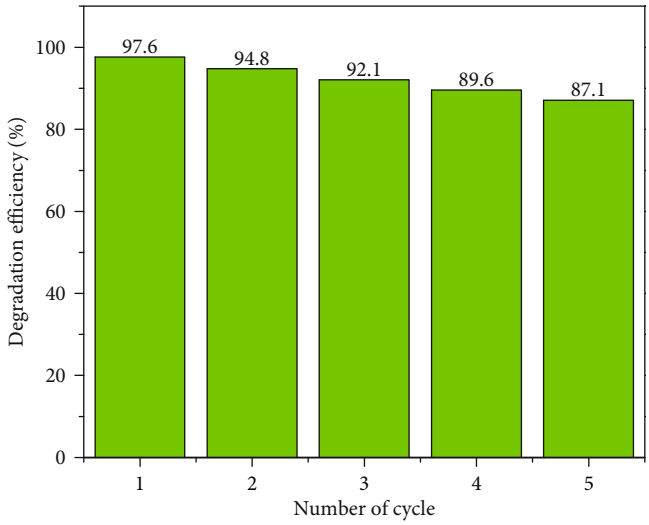

Figure 7: Photostability of ZnO-GO nanocomposites for MB degradation for five cycles.

$k = 0.0397\ \text{min}^{-1}$. Also, Raghavan et al. [48] performed the photocatalytic degradation of MB by reduced graphene oxide/titanium dioxide/zinc oxide (rGO/TiO_2/ZnO) ternary nanocomposites; the intermixture was irradiated with a 300 W xenon lamp; TiO_2, rGO/TiO_2, and rGO/TiO_2/ZnO degraded 92%, 68%, and 47% MB, respectively, after 120 min irradiation. The above studies are comparable to our work; the ZnO-GO composites used for photodegradation of MB in the our present work are smaller sheets, and the experimental system is irradiated by a lower-power (50 W) Hg lamp.

According to the results of these photocatalytic experiments, the degradation process of MB dyes with ZnO and ZnO-GO was studied in details, which fits the first-order reaction kinetics.

$$\begin{aligned} \frac{-dC}{dt} &= k \times C, \\ -\ln\left(\frac{C}{C_0}\right) &= k \times t, \\ \ln\left(\frac{C_0}{C}\right) &= kt, \end{aligned} \tag{2}$$

where C_0 and C represent the initial concentration and the concentration at a time interval of 10 min, respectively, t is

the irradiation time, and k (min^{-1}) denotes the first-order rate constant. Figure 6(c) reveals a profile depicting linear relationship between $\ln(C_0/C)$ and degradation time (t) under UV light irradiation. For the ZnO-GO nanocomposites prepared by adding of 100 mg of GO and being annealed at 450°C, the value of the first-order rate constant, k, for MB degradation is 0.04401 min^{-1}, while that is 0.03096 min^{-1} for ZnO-GO nanocomposites without annealing treatments. k values for the blank photocatalysis and ZnO crystals are 0.00074 min^{-1} and 0.02378 min^{-1}, respectively. $R^2 > 0.9$ in all MB degradation experiments indicates that the photocatalytic degradation of MB adheres to the pseudo first-order reaction. Therefore, the annealed ZnO-GO catalyst containing 100 mg of GO exhibits the fastest photocatalytic rate for MB degradation under ultraviolet and visible light illumination.

The reusability and photostability of ZnO-GO nanocomposites containing 100 mg GO were investigated for MB degradation for five cycles. The ZnO-GO catalysts were collected and washed for next cycle degradation. The obtained powder was dried at 60°C for 12 h. The photodegradation efficiencies for five cycles are shown in Figure 7. High photostability for MB degradation with efficiencies of 97.6, 94.8, 92.1, 89.6, and 87.1% was found for five cycles, respectively. This shows that ZnO-GO nanocomposites prepared by a precipitation method having outstanding reusability and photostability. These results may be assigned to the chemical stability of the ZnO-GO nanocomposites and their excellent photoelectric performance.

4. Conclusions

In this work, the ZnO-GO nanocomposites were successfully synthesized via a precipitation method, where GO sheets are used as the catalysis carrier. The functional groups of GO provide anchor sites for the growth cross-linked ZnO nanoflakes on the surface of GO. With the help of comprehensive characterization by means of XRD, XPS, and SEM, it can conclude that the ZnO has been successfully decorated on the surface of GO. The photodegradation of MB dye from water with the prepared nanocomposite was also studied. We demonstrated that the annealed ZnO-GO nanocomposites exhibited better efficient photocatalytic activity than that from pure ZnO. Under the optical conditions, the degradation rate reaches to 97.6% within 90 min, and the first-order rate constant, k, is 0.04401 min^{-1}. This effective photocatalyst is an outstanding candidate for catalysts in photocatalytic degradation of organic dyes.

Data Availability

The data used to support the findings of this study are included within the article. If the readers need specific original data, please contact Mr. Lin (E-mail: ly49871@163.com).

Conflicts of Interest

The authors declare that there is no conflict of interest regarding the publication of this article.

Acknowledgments

This research was financially supported by the National Natural Science Foundation of China (NSFC) (No. 21246002), the Minjiang Scholarship of Fujian Province (No. MinGaojiao[2010]-117), the Central Government Guided Fund for Local Economic Development (No. 830170778), the R&D Fund for Strategic Emerging Industry of Fujian Province (No. 82918001), the International Cooperation Project of Fujian Science and Technology Department (No. 830170771), and the Teaching and Researching Fund for Young Staff of Fujian Educational Department (No. JT180040).

Supplementary Materials

Figure 1: decreasing trend in the diffraction peaks intensity of ZnO (a) and ZnO-GO (b). Figure 2: the C/C_0 of MB vs. time in the dark and under UV light. Figure 3: SEM image of ZnO-GO with higher concentration of GO. *(Supplementary Materials)*

References

[1] Ā. A. Bāzghale and A. Mohammad-khāh, "Sonocatalytic decolorization of methylene blue from aqueous media by La:ZnO/GO nanocomposites," *Research on Chemical Intermediates*, vol. 45, no. 4, pp. 1985–2005, 2019.

[2] A. Kudo and Y. Miseki, "Heterogeneous photocatalyst materials for water splitting," *Chemical Society Reviews*, vol. 38, no. 1, pp. 253–278, 2009.

[3] A. Fujishima and K. Honda, "Electrochemical photolysis of water at a semiconductor electrode," *Nature*, vol. 238, no. 5358, pp. 37-38, 1972.

[4] B. Siripireddy and B. K. Mandal, "Facile green synthesis of zinc oxide nanoparticles by *Eucalyptus globulus* and their photocatalytic and antioxidant activity," *Advanced Powder Technology*, vol. 28, no. 3, pp. 785–797, 2017.

[5] D. Hong, G. Cao, X. Zhang et al., "Construction of a Pt-modified chestnut-shell-like ZnO photocatalyst for high-efficiency photochemical water splitting," *Electrochimica Acta*, vol. 283, pp. 959–969, 2018.

[6] S. Nagamine and K. Inohara, "Photocatalytic microreactor using anodized TiO_2 nanotube array," *Advanced Powder Technology*, vol. 29, no. 12, pp. 3100–3106, 2018.

[7] A. Pruna, Z. Wu, J. A. Zapien, Y. Y. Li, and A. Ruotolo, "Enhanced photocatalytic performance of ZnO nanostructures by electrochemical hybridization with graphene oxide," *Applied Surface Science*, vol. 441, pp. 936–944, 2018.

[8] H. Wang, S. Baek, J. Lee, and S. Lim, "High photocatalytic activity of silver-loaded ZnO-SnO_2 coupled catalysts," *Chemical Engineering Journal*, vol. 146, no. 3, pp. 355–361, 2009.

[9] S. Yan, Z. Liu, X. Wei et al., "Preparation and photoelectrochemical properties of CdS nanoparticles using supercritical carbon dioxide," *Journal of Nanoscience and Nanotechnology*, vol. 16, no. 7, pp. 7203–7209, 2016.

[10] E. Soignard, D. Machon, P. F. McMillan, J. Dong, B. Xu, and K. Leinenweber, "Spinel-structured gallium oxynitride (Ga_3O_3N) synthesis and characterization: an experimental and theoretical study," *Chemistry of Materials*, vol. 17, no. 22, pp. 5465–5472, 2005.

[11] F. G. Rinaldi, A. F. Arif, T. Ogi, K. Okuyama, and E. Tanabe, "Strong metal-support interactions (SMSIs) between Pt and Ti^{3+} on Pt/TiO_x nanoparticles for enhanced degradation of organic pollutant," *Advanced Powder Technology*, vol. 28, no. 11, pp. 2987–2995, 2017.

[12] J. H. Li, R. Y. Hong, M. Y. Li, H. Z. Li, Y. Zheng, and J. Ding, "Effects of ZnO nanoparticles on the mechanical and antibacterial properties of polyurethane coatings," *Progress in Organic Coatings*, vol. 64, no. 4, pp. 504–509, 2009.

[13] R. Y. Hong, J. H. Li, L. L. Chen et al., "Synthesis, surface modification and photocatalytic property of ZnO nanoparticles," *Powder Technology*, vol. 189, no. 3, pp. 426–432, 2009.

[14] P. Zhang, R. Y. Hong, Q. Chen, and W. G. Feng, "On the electrical conductivity and photocatalytic activity of aluminum-doped zinc oxide," *Powder Technology*, vol. 253, no. 2, pp. 360–367, 2014.

[15] S. Singhal, S. Dixit, and A. K. Shukla, "Self-assembly of the Ag deposited ZnO/carbon nanospheres: a resourceful photocatalyst for efficient photocatalytic degradation of methylene blue dye in water," *Advanced Powder Technology*, vol. 29, no. 12, pp. 3483–3492, 2018.

[16] W. Han, L. Ren, X. Qi et al., "Synthesis of CdS/ZnO/graphene composite with high-efficiency photoelectrochemical activities under solar radiation," *Applied Surface Science*, vol. 299, pp. 12–18, 2014.

[17] S. M. Yakout and A. M. El-Sayed, "Enhanced ferromagnetic and photocatalytic properties in Mn or Fe doped p-CuO/n-ZnO nanocomposites," *Advanced Powder Technology*, vol. 30, no. 11, pp. 2841–2850, 2019.

[18] Y. T. Kwon, S. O. Kang, J. A. Cheon, Y. Song, J. J. Lee, and Y. H. Choa, "Fabrication of a graphene/ZnO based p-n junction device and its ultraviolet photoresponse properties," *Applied Surface Science*, vol. 415, pp. 2–7, 2017.

[19] Y. Zhao, L. Liu, T. Cui, G. Tong, and W. Wu, "Enhanced photocatalytic properties of ZnO/reduced graphene oxide sheets (rGO) composites with controllable morphology and composition," *Applied Surface Science*, vol. 412, pp. 58–68, 2017.

[20] S. Ameen, M. Shaheer Akhtar, H. K. Seo, and H. Shik Shin, "Advanced ZnO-graphene oxide nanohybrid and its photocatalytic applications," *Materials Letters*, vol. 100, pp. 261–265, 2013.

[21] B. Xue and Y. Zou, "High photocatalytic activity of ZnO-graphene composite," *Journal of Colloid and Interface Science*, vol. 529, pp. 306–313, 2018.

[22] J. H. Feng, F. Li, X. Li et al., "An amplification label of core-shell CdSe@CdS QD sensitized GO for a signal-on photoelectrochemical immunosensor for amyloid β-protein," *Journal of Materials Chemistry B*, vol. 7, no. 7, pp. 1142–1148, 2019.

[23] Y. Bu, Z. Chen, W. Li, and B. Hou, "Highly efficient photocatalytic performance of graphene-ZnO quasi-shell-core composite material," *ACS Applied Materials & Interfaces*, vol. 5, no. 23, pp. 12361–12368, 2013.

[24] L. L. Zhang, X. Zhao, M. D. Stoller et al., "Highly conductive and porous activated reduced graphene oxide films for high-power supercapacitors," *Nano Letters*, vol. 12, no. 4, pp. 1806–1812, 2012.

[25] M. M. Mohamed, M. A. Ghanem, M. Khairy, E. Naguib, and N. H. Alotaibi, "Zinc oxide incorporated carbon nanotubes or graphene oxide nanohybrids for enhanced sonophotocatalytic degradation of methylene blue dye," *Applied Surface Science*, vol. 487, pp. 539–549, 2019.

[26] A. E. Hamidi, K. Meziane, A. E. Hichou et al., "Refractive index controlled by film morphology and free carrier density in undoped ZnO through sol-pH variation," *Optik*, vol. 158, pp. 1139–1146, 2018.

[27] M. A. Hernández-Carrillo, R. Torres-Ricárdez, M. F. García-Mendoza et al., "Eu-modified ZnO nanoparticles for applications in photocatalysis," *Catalysis Today*, vol. 349, pp. 191–197, 2020.

[28] Y. Wu, L. Zhang, Y. Zhou et al., "Light-induced ZnO/Ag/rGO bactericidal photocatalyst with synergistic effect of sustained release of silver ions and enhanced reactive oxygen species," *Chinese Journal of Catalysis*, vol. 40, no. 5, pp. 691–702, 2019.

[29] C. Xu, X. Wang, and J. Zhu, "Graphene-metal particle nanocomposites," *Journal of Physical Chemistry C*, vol. 112, no. 50, pp. 19841–19845, 2008.

[30] B. Straumal, A. Mazilkin, S. Protasova et al., "Influence of texture on the ferromagnetic properties of nanograined ZnO films," *Physica Status Solidi (b)*, vol. 248, no. 7, pp. 1581–1586, 2011.

[31] M. de Sousa, C. H. Z. Martins, L. S. Franqui et al., "Covalent functionalization of graphene oxide withd-mannose: evaluating the hemolytic effect and protein corona formation," *Journal of Materials Chemistry B*, vol. 6, no. 18, pp. 2803–2812, 2018.

[32] Y. Haldorai, W. Voit, and J. J. Shim, "Nano ZnO@reduced graphene oxide composite for high performance supercapacitor: green synthesis in supercritical fluid," *Electrochimica Acta*, vol. 120, pp. 65–72, 2014.

[33] M. Ahmad, E. Ahmed, Z. L. Hong et al., "A facile one-step approach to synthesizing ZnO/graphene composites for enhanced degradation of methylene blue under visible light," *Applied Surface Science*, vol. 274, no. 1, pp. 273–281, 2013.

[34] K. Kotsis and V. Staemmler, "*Ab initio* calculations of the O1s XPS spectra of ZnO and Zn oxo compounds," *Physical Chemistry Chemical Physics*, vol. 8, no. 13, pp. 1490–1498, 2006.

[35] S. Pal, N. Gogurla, A. Das et al., "Clustered vacancies in ZnO: chemical aspects and consequences on physical properties," *Journal of Physics D Applied Physics*, vol. 51, no. 10, p. 105107, 2018.

[36] I. Chowdhury, M. C. Duch, N. D. Mansukhani, M. C. Hersam, and D. Bouchard, "Interactions of graphene oxide nanomaterials with natural organic matter and metal oxide surfaces," *Environmental Science & Technology*, vol. 48, no. 16, pp. 9382–9390, 2014.

[37] S. Hernández, D. Hidalgo, A. Sacco et al., "Comparison of photocatalytic and transport properties of TiO_2 and ZnO nanostructures for solar-driven water splitting," *Physical Chemistry Chemical Physics*, vol. 17, no. 12, pp. 7775–7786, 2015.

[38] X. Huang, Z. Yin, S. Wu et al., "Graphene-based materials: synthesis, characterization, properties, and applications," *Small*, vol. 7, no. 14, pp. 1876–1902, 2011.

[39] S. Park, K.-S. Lee, G. Bozoklu, W. Cai, S. B. T. Nguyen, and R. S. Ruoff, "Graphene oxide papers modified by divalent ions-enhancing mechanical properties *via* chemical cross-linking," *ACS Nano*, vol. 2, no. 3, pp. 572–578, 2008.

[40] C. Cheng, S. Nie, S. Li et al., "Biopolymer functionalized reduced graphene oxide with enhanced biocompatibility *via*

mussel inspired coatings/anchors," *Journal of Materials Chemistry B*, vol. 1, no. 3, pp. 265–275, 2013.

[41] X. Ma and Z. Wang, "The optical properties of rare earth Gd doped ZnO nanocrystals," *Materials Science in Semiconductor Processing*, vol. 15, no. 3, pp. 227–231, 2012.

[42] J. J. Schneider, R. C. Hoffmann, J. Engstler et al., "A printed and flexible field-effect transistor device with nanoscale zinc oxide as active semiconductor material," *Advanced Materials*, vol. 20, no. 18, pp. 3383–3387, 2008.

[43] K. Huang, Y. H. Li, S. Lin et al., "A facile route to reduced graphene oxide-zinc oxide nanorod composites with enhanced photocatalytic activity," *Powder Technology*, vol. 257, pp. 113–119, 2014.

[44] C. Ye, Y. Bando, G. Shen, and D. Golberg, "Thickness-dependent photocatalytic performance of ZnO nanoplatelets," *Journal of Physical Chemistry B*, vol. 110, no. 31, pp. 15146–15151, 2006.

[45] S. Verma, B. T. Rao, J. Jayabalan et al., "Studies on growth of Au cube-ZnO core-shell nanoparticles for photocatalytic degradation of methylene blue and methyl orange dyes in aqueous media and in presence of different scavengers," *Journal of Environmental Chemical Engineering*, vol. 7, no. 4, p. 103209, 2019.

[46] M. Vanitha, S. V. Keerthi, and N. Balasubramanian, "Visible light photocatalysis of methylene blue by graphene-based ZnO and Ag/AgCl nanocomposites," *Desalination and Water Treatment*, vol. 54, no. 10, pp. 2748–2756, 2015.

[47] L. Ling, Y. Wang, W. Zhang, Z. Ge, W. Duan, and B. Liu, "Preparation of a novel ternary composite of TiO_2/UiO-66-NH_2/graphene oxide with enhanced photocatalytic activities," *Catalysis Letters*, vol. 148, no. 7, pp. 1978–1984, 2018.

[48] N. Raghavan, S. Thangavel, and G. Venugopal, "Enhanced photocatalytic degradation of methylene blue by reduced graphene-oxide/titanium dioxide/zinc oxide ternary nanocomposites," *Materials Science in Semiconductor Processing*, vol. 30, pp. 321–329, 2015.